Smarter Temperature Setup for Reflow Oven to Minimize Temperature Variation Among Components

Yangyang Lai, *Graduate Student Member, IEEE*, Ke Pan, *Graduate Student Member, IEEE*, Chongyang Cai, Pengcheng Yin, Junbo Yang, and Seungbae Park, *Senior Member, IEEE*

***Abstract*— The thermomechanical reliability of surface mount components (SMCs) is closely related to the reflow soldering process. With the rise of board complexity, an optimal reflow profile must consider the mix of large and small components, the density of the components on the board, and the board dimensions. It has been a significant challenge to achieve uniform temperature on SMCs with different sizes and different thermal masses, such as capacitors, transistors, quad-flat no-leads (QFN), and ball grid array (BGA) packages. To reflow large components such as BGA packages, the minimum reflow temperature should be reached, meanwhile, the temperature should not exceed the damaging temperature of the smaller or heat-sensitive components. The recommended reflow profile is defined as a band or process window. To achieve good quality soldering, the temperature applied to the solder under varied sizes of components should be within the recommended band. This article introduces a numerical method based on a compact model to predict the reflow profile for bulky BGA packages. The impinging gas temperature is used as the boundary condition to predict the temperature distribution throughout a board with different sized components. The proper oven temperature setting to achieve the ideal profiles is obtained finally.**

***Index Terms*— Compact model, computational fluid dynamics (CFDs), reflow soldering process, surface-mount technology.**

I. Introduction

THE reflow soldering process is of vital importance to forming robust solder joints under surface mount components (SMCs). Convective heating technology is preferred over infrared radiation because of the better temperature uniformity [1], [2]. However, uneven temperature distribution occurs (during convective heating technology, such as reflow) in large printed circuit board (PCB) assemblies with different sizes of SMCs [3]. Therefore, the actual temperature of solder joints in different SMCs may vary from the desired reflow profile, which can cause various assembly defects [4]. Incomplete flux's cleaning action and non-reflowed or partially reflowed soldering caused by insufficient heating can cause a rough or lumpy surface finish of a solder joint. Premature flux activation caused by excessive heating can result in solder paste drying before forming solder joints. Poor-quality soldering can cause solder joint failures (e.g., skewing, bridging, voiding, and insufficient wetting), and it can result in electronic device reliability issues or prevent them from functioning [5], [6]. Reflow soldering needs to be considered in the early stage of package and board design [7].

A reflow profile consists of six output parameters including ramp profile rate, soak zone duration, soak zone temperature range, time above liquidus (TAL), peak temperature, and cooling ramp rate. Without a predictive numerical model, a large amount of trial tests is needed to obtain these six output parameters. Moreover, reflow profiles are usually collected by thermocouples attached to the surface of packages or PCB, which cannot represent the real temperature of the solder joints during the reflow process. However, the temperature of solder joints under the components is of significant interest but is hard to measure directly. For small-size components, the surface temperature may reflect their solder performance approximately. Whereas, solder joint temperatures of bulky components, such as ball grid array (BGA) packages, are commonly lower than their surface temperature. Even the temperature of the solder joint at the center of the package is much lower than at the periphery. Therefore, an accurate assessment is needed to optimize the reflow profile of different boards.

The multiple reflow technique is commonly used to reflow bulky BGA packages with big thermal mass [8]. However, a side effect of the growth of the intermetallic compound (IMC) layer is the reliability issue arise unless a thin, uniform IMC layer forms in solder joints [9]. A thick IMC layer can bring adverse effects because its brittle nature can cause early mechanical failure [10]. Therefore, the reflow temperature setting compatible with all components on the board is necessary.

The optimization of reflow profiles has been extensively studied. Illés and Harsányi [1] investigated the heat transfer characteristics that are affected by the construction of the reflow oven and proposed that the changing of heat transfer coefficient of impinging gas was highly correlated with the height of measurement spotsClick or tap here to enter text. Esfandyari *et al.* [11] applied FEM to simulate the reflow soldering process in an over-pressurized oven. In his sim-

Manuscript received August 30, 2021; revised January 2, 2022; accepted February 21, 2022. Date of publication February 24, 2022; date of current version March 28, 2022. Recommended for publication by Associate Editor Z. Zhou upon evaluation of reviewers' comments. *(Corresponding author: Yangyang Lai.)*

The authors are with the Department of Mechanical Engineering, State University of New York at Binghamton, Binghamton, NY 13902 USA (e-mail: ylai9@binghamton.edu).

Color versions of one or more figures in this article are available at https://doi.org/10.1109/TCPMT.2022.3153952.

Digital Object Identifier 10.1109/TCPMT.2022.3153952

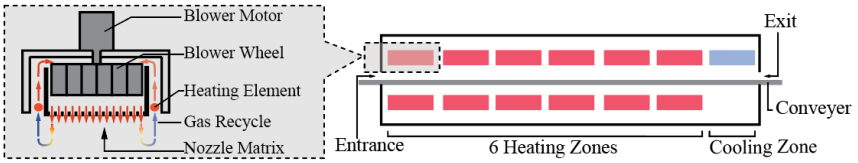

Fig. 1. Schematic of the reflow oven.

ulation, he investigated the void fraction of solder material influenced by oven parameter settings. Tsai [12] proposed a well-designed system using artificial intelligence (AI) methods to study the relationship between the input factors including the settings of the reflow oven, board configuration, and flow speed and heating responses of reflow profiles. A genetic algorithm was used to optimize thermal profiling factors. However, that method requires many experiments, which was costly. Lai *et al.* [13] and [14] investigated the temperature of solder joints under varied size component using computational fluid dynamic (CFD) simulation. Lau *et al.* [15] used a CFD model to analyze the temperatures of solder balls of a BGA assembly during the reflow soldering processClick or tap here to enter text. In Lau's research, board-level analysis and the dynamic movement of BGA assembly were ignored. Shao *et al.* [16] used the CFD model to obtain the working temperature distribution of a 2.5-D package and mapped it to an FEA model to observe warpage. Deng *et al.* [17] used a CFD model to predict the temperature distribution of the system in package assembly during the reflow soldering process. Straubinger *et al.* [18] studied the relationship between heat distribution and the thickness of different circuit boards analyticallyClick or tap here to enter text. However, solder joint temperature as significant importance to reliability was not considered by Deng or Straubinger.

In this study, a CFD model is used to simulate the reflow process of BGA packages in a typical six-zone convective reflow oven. By using an airflow model simulating the oven environment and appropriate boundary conditions, the temperature distribution within a BGA package has been obtained. Considering the variation of package structures, a compact modeling method is summarized for lidded and lidless BGA packages. The boundary condition used in package level simulation will be used to board-level simulation. Temperature variation within and outside the BGA packages is observed. Reflow profile is not a single line, but a band or process window. The best reflow profile does not specify a particular temperature curve but allows a band or process window. All the solder temperatures under the various components should remain within the window. This study will be beneficial to reflow profile control for complex PCB assembly, especially with bulky BGA packages.

II. Modeling Development and Validation

A. Configuration of Reflow Oven

A six-zone forced convection reflow oven as shown in Fig. 1 was used in the experiments. PCB assemblies were conveyed through the six heating zones and then one cooling zone. Each heating zone plenum is topped by a blower motor.

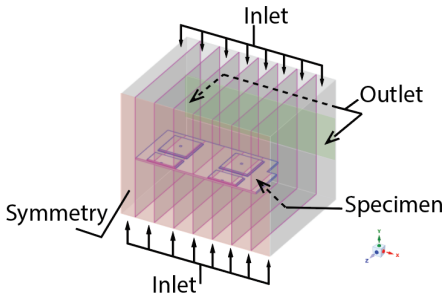

Fig. 2. Schematic of the CFD model.

Compressed gas is pulled upward past heating elements by the blower, which then pushes the hot gas downward through a matrix of nozzles onto the PCB traveling on the conveyor. There are two reference setpoints: percent voltage for the heating element and heating zone temperature. If the zone temperature is at the correct temperature, then heating elements will be kept at their setpoints. If zone temperature is over the preset temperature, heating elements will decrease in intensity. If zone temperature is under the preset temperature, heating elements will operate at a level greater than their setpoints. Heating elements are modified only enough to compensate for the heat transfer deviation. Using this closed-loop control, the ability to repeat a product temperature profile can be achieved.

B. Model Geometry and Boundary Condition

As shown in Fig. 2, the specimen is created in the center of the fluid domain, which appears semi-transparent for easy visualization. There are six identical BGA packages on the 110 mm × 120 mm × 1.6 mm PCB. Half symmetry is used to save computational time. A 26 × 26 mm^2 bare die is attached to the top of each package. SAC305 (96.5 Sn/3.0 Ag/0.5 Cu) solder was used as the interconnection between packages and PCB. Eight separate gas inlets on the top and bottom of the fluid domain allow precise control of the gas temperature.

Considering the movement of the specimen inside the reflow oven, eight temperature profiles are assigned to inlets individually. Each profile shares the same trajectory but with an incremental delay time t_{delay} that is associated with the conveyor speed v, and the spacing of each two adjacent inlets s_{inlet}, as shown in the following equation:

$$t_{\text{delay}} = n s_{\text{inlet}} / v. \tag{1}$$

To observe the board temperature changing in the reflow process, the temperature contours were exported as shown in Fig. 3.

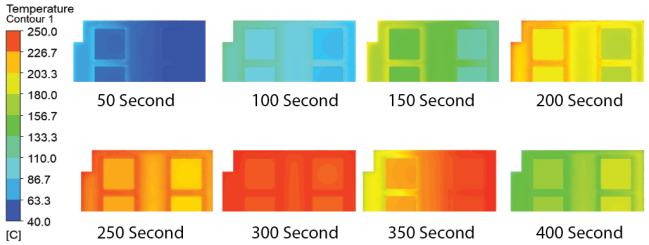

Fig. 3. Board temperature contours.

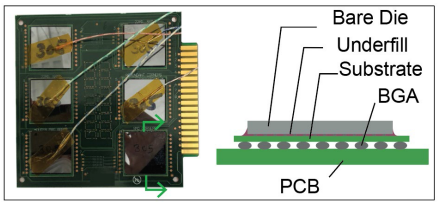

Fig. 4. BGA package specimen and thermocouple attachment.

TABLE I
TEMPERATURE SETTING FOR HEATING ZONES

Zone	1	2	3	4	5	6
Temperature (°C)	100	140	155	170	240	260

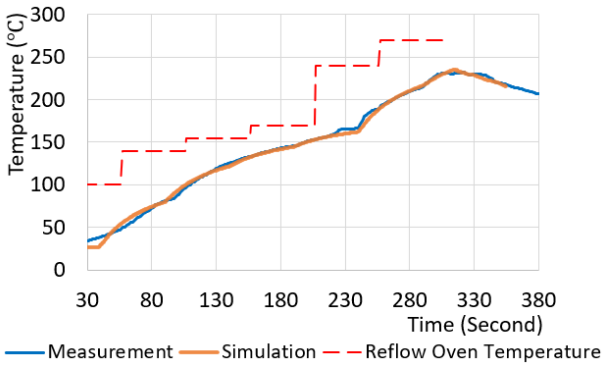

Fig. 5. Experiment and simulation results.

C. Experiment for Validation

K-type thermocouples were attached to the center of each bare die surface using thermal tapes (see Fig. 4). A six-channel thermal profiler with a thermal barrier cover was used to collect in-transit temperature data during reflow.

The temperature of each zone was preset according to Table I. The dwell time of each heating zone was determined by conveyor speed. In this experiment, the conveyor speed was set as 5.6 mm/s to reach a 300-s heating duration.

An anemometer was used to measure the velocity of the impinging gas. The variation of gas velocity was found locationally within each heating zone because of the varied relative position of each nozzle to the blower wheel. The gas velocity was adjusted within the field measurement result range in the numerical model.

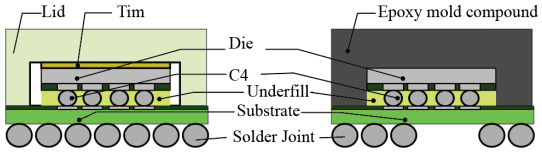

Fig. 6. Lidded and lidless packages.

Fig. 5 shows the simulation result which is in good agreement with the experimental results. The difference at the peak temperature is 0.9 °C. The maximum ramp rate difference is 1.33 °C/s. Boundary condition independence was considered in the model validation. Simulation results and experimental results match well with two other sets of reflow oven temperatures. In addition to the component surface temperature, the solder joint temperature can be obtained simultaneously based on the model.

III. COMPACT MODEL GENERATION

The compact model approach described in this study relies on thermophysical property simplifications to generate efficient models without the expense and time needed to use the detailed models. Small and thin features such as leads, thermal interface material (TIM), through silicon via and micro-bumps are the reasons why it is not practical to use detailed models of microelectronic packages in system-level simulation.

Lidded and lidless packages as two typical packaging methods for bulky components are both studied as shown in Fig. 6. Lidded packages are protected by a metal lid on the top that dissipates heat to the outside cooler. Another way is to use the epoxy molding compound (EMC) to encapsulate the delicate microelectronics [19].

The density and specific heat of lumped composites are determined by the following equations [20]:

$$\rho_{\text{eff}} = \frac{\sum \rho_i V_i}{\sum V_i} \tag{2}$$

$$C_{\text{eff}} = \frac{\sum C_{p,i} m_i}{\sum m_i}. \tag{3}$$

Based on the orientation of the materials of the composite entities, heat transfer pathways can be identified as resistances in parallel and series. Orthotropic effective conductivities can be defined by the following equations:

$$K_{\text{eff}} = \sum \frac{K_i A_i}{A_{\text{total}}} \tag{4}$$

$$K_{\text{eff}} = \sum \frac{t_{\text{total}}}{\sum \frac{t_i}{K_i}}. \tag{5}$$

An error analysis of three different model simplifications is conducted using the following equation:

$$\text{Error} = \frac{T_{\text{compact}} - T_{\text{detail}}}{T_{\text{detail}} - T_0}. \tag{6}$$

Three differentsimplification models for lidded packages are presented in Fig. 7. The detailed model is treated as the reference for error analysis.

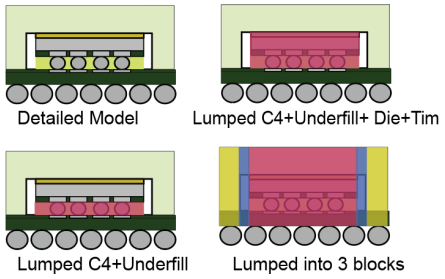

Fig. 7. Detailed model and compact models for lidded package.

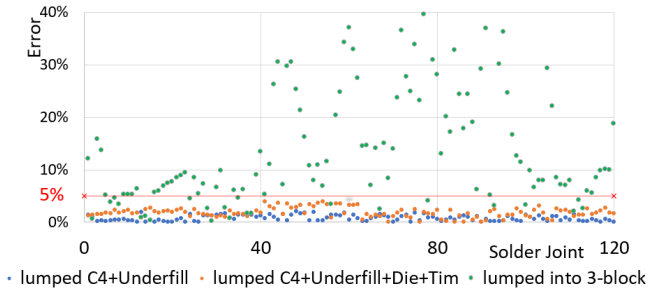

Fig. 8. Error plot of three compact models for lidded package.

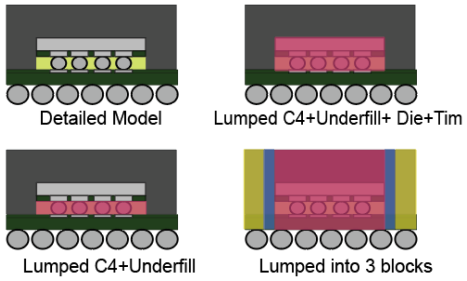

Fig. 9. Detailed model and compact models for lidless package.

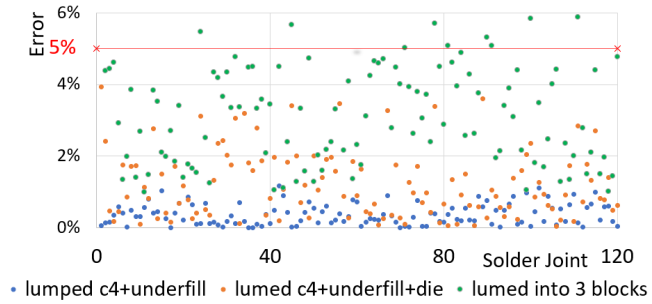

Fig. 10. Error plot of three compact models for lidless package.

The boundary condition of all the models is to heat components using 227 °C impinging gas lasting 50 s. The terminal temperatures of the solder joints are compared.

The error plot of three compact models is shown in Fig. 8. Only the model lumped into three blocks produces an error that exceeds the acceptable range, 5% [20].

Three different simplification methods for lidless packages are present in Fig. 9. The significant difference from lidded packages is the mold compound wrapping the entire unit.

TABLE II
MATERIAL PROPERTIES USED FOR SIMULATION [22], [23]

Material		Thermal Conductivity (W/m.K)	Specific Heat (J/kg.K)	Density (kg/m³)
Air	27°C	0.0263	1007	1.1614
	77°C	0.0300	1009	0.9950
	127°C	0.0338	1014	0.8711
	177°C	0.0373	1021	0.7740
	227°C	0.0407	1030	0.6964
	277°C	0.0439	1040	0.6329
Silicon		98.4	721	2300
PCB		0.2900	1450	1859
SAC 305	solid	-0.007105*T+70.52	0.22+0.000134*T-1642*T^2	7400
	mushy	$k_l + \frac{k_s - k_l}{T_l - T_s}(T_l - T)$	$C_{pl} + \frac{C_{ps} - C_{pL}}{T_l - T_s}(T_l - T)$	8000
	liquidus	25	259	8000

The error plot of three compact models is shown in Fig. 10. Only the model lumped into three blocks produces errors over 5%. The results of two other compact models are in the safe range.

To maximize computation efficiency, the simplest model should be used once the error is within the acceptable range. From the error analysis, the component is recommended to be divided into three parts. The upper part is the lid or mold compound corresponding to two packaging types. Core portions including Die, C4, and Underfill should be lumped into a single block. The remaining part is the substrate on the bottom of the component.

IV. CFD SIMULATION FOR VARIED SIZE COMPONENT

A. Reflow Temperature for Bulky BGA Packages

With the methodology of compacting the model, a simulation for bulky packages can be started. A series of discrete control volumes were generated based on model geometry using ANSYS-Fluent. The transient model solver was used with pressure-based type and K-epsilon turbulence. The material property of the air was set in polynomial equations of temperature. To consider the effect of latent heat during the solder phase transition, pure solvent melting heat was set to 53.08 J/g. Solidus and liquidus temperatures of SAC solder were set to 217 °C and 220 °C, respectively [21]. The thermal properties of the remaining items are listed in Table II.

For bulky BGA packages, solder joints in the diagonal direction were monitored in the reflow process where both hot and cold spots were included. To ensure good soldering quality, the minimum reflow temperature should be reached in the coldest spot, which is always at the center of the BGA or under the gap between the lid and the die. Because of the geometric characteristic of BGA packages, half or quarter symmetry can be used to speed up computation, which is unlikely in board-level simulation. This also shows the necessity to put the study of BGA packages ahead of the complete board assembly.

To find a set of proper oven temperatures, multiple trials are inevitable. Lumped system analysis was used to determine the increment or reduction of inlet gas temperature as a reference

$$hA(T_\infty - T(t))dt = mC_p dT \tag{7}$$

TABLE III
REFLOW PARAMETER RECOMMENDATION FOR SAC305 [24]

Reflow Profile Parameter	Recommended	Acceptable
Ramp Profile Rate (Average Ambient to Peak)	0.5–1 °C/second	0.5–2.5 °C/second
soak zone duration	30–90 seconds	30–120 seconds
soak zone temperature	160–180 °C	150–200 °C
time above liquidus (TAL)	45–60 seconds	30–100 seconds
peak temperature	230–260 °C	230–262 °C
cooling ramp rate	2–6 °C/second	0.5–6 °C/second

where h is the convective heat transfer coefficient, A is surface area, m is the mass of the component, C_p is the specific heat capacity, and T_∞ is the inlet gas temperature. dT in (2) is equal to $d(T(t) - T_\infty)$, we find

$$\frac{d(T(t) - T_\infty)}{T(t) - T_\infty} = -\frac{hA}{mC_p}dt \tag{8}$$

$$\frac{T(t) - T_\infty}{T_i - T_\infty} = e^{-bt} \tag{9}$$

where b is equal to (hA/mC_p). From the equations above, the relation between component temperature and ambient temperature is established. The duration of the component staying in each zone is 45 s as a constant. T_i is known as the initial component temperature before entering a heating zone. The temperature difference between inlet gas temperature T_∞ and $T(0)$ can determine $T(45)$, which is the terminal temperature in that zone. However, the comprehensive computation by CFD modeling is required because the interaction of interior and external conduction between component and PCB are ignored in this method.

B. Reflow Profiling for Varied Size Components

The solder joint temperature of a lidded BGA package in the reflow process was studied using the method introduced above. After several trials, the minimum reflow temperature was reached in the cold spot which was under the gap between the lid and core portion. The peak temperature is 230 °C and the TAL reaches 30 s. The hot spot, which is at the peripheral of the BGA also in the safe range. Its peak temperature is 247 °C and the TAL is 45 s. According to the reflow parameter recommendation from the solder paste company shown in Table III, the performance of this bulky BGA package is qualified.

The PCB assembly used in board-level simulation consists of three different-sized components as shown in Fig. 11. Besides package A, a smaller package B, and the resistors are on the board. Inlet gas temperatures of the six heating zones are in Table IV, which allow package A to form the qualified reflow profiles. To ensure the soldering quality of all the types of components, the risk of overheating for package B and resistors are needed to be eliminated.

The solder temperature profiles of all three components are shown in Figs. 12–14. The yellow stepped lines in the plots are the inlet gas temperatures as the boundary condition of the simulation.

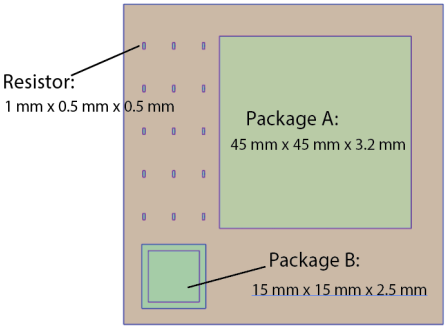

Fig. 11. Dimensions of two packages and passive resistors.

TABLE IV
TEMPERATURE SETTING FOR LINEAR RAMP PROFILE

Zone	1	2	3	4	5	6
Temperature (°C)	100	150	165	210	250	260

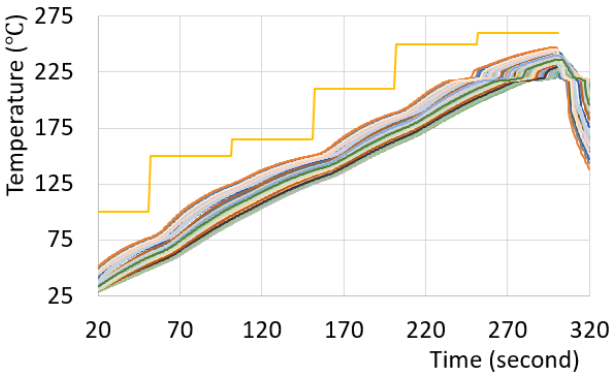

Fig. 12. Solder temperature of package A.

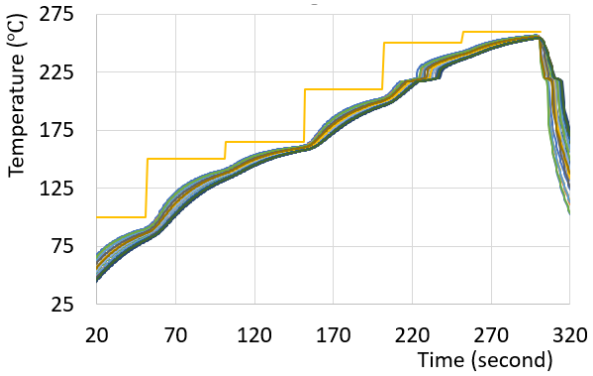

Fig. 13. Solder temperature of package B.

The plateaus in each profile imply the solder experiences complete melting and solidification. The ramp rate, which is the slope of temperature versus time for the heating section of the complete profile, is 0.77 °C/s–0.81 °C/s. For package B and the resistors, TAL is in the range of 74–86 s, which is long enough for the flux to evaporate and to accomplish metallurgical bonding of solder and pads. However, these values fall within the acceptable range, but out of the recommended

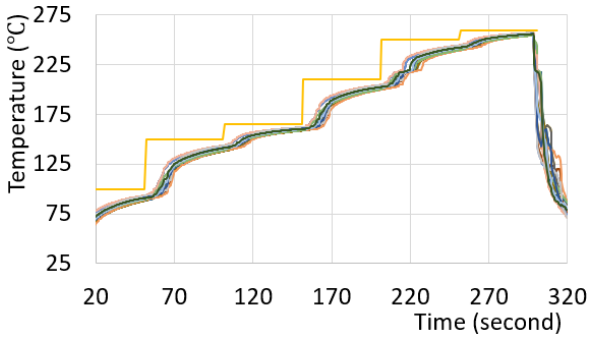

Fig. 14. Solder temperature of resistors.

TABLE V
TEMPERATURE SETTING FOR RAMP-SOAK-SPIKE PROFILE

Zone	1	2	3	4	5	6
Temperature (°C)	145	195	195	195	254	260

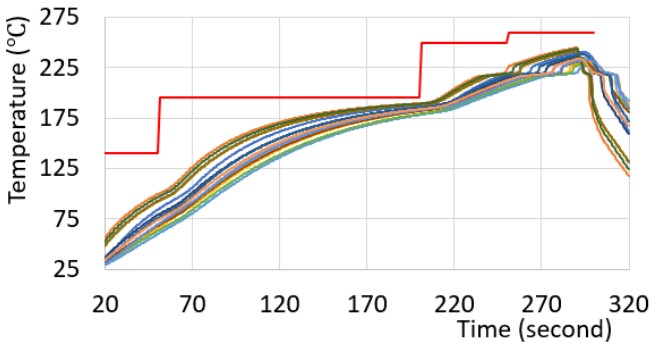

Fig. 15. Updated solder temperature of package A.

range. The peak temperatures vary from 253 °C to 258 °C, which are in the safe range.

C. Update to Soak Profile

The previous thermal profiles are the ramp-to-peak profiles, which are also called tent profiles. It is a linear ramp to the max temperature. For the PCB assembly with a big thermal mass differential, the ramp-soak-spike profile is used to bring the temperature of all components on the PCB assembly to equilibrium before they reach the reflow section so that all parts of the PCB assembly will be reflowed simultaneously. A PCB assembly with bulky components, such as BGA packages, is recommended for being reflowed under a soak profile.

To update boundary conditions, Zone 3 and Zone 4 are treated as the soak zones. The inlet temperatures of six zones are set as shown in Table V, with no changes to Zone 6 as it is at the limit of the component bearable temperature.

As shown in Figs. 15–17, the solder joint temperatures of package B and the resistors are closed to or even reach the inlet temperature (the red color stepped lines) in the soak zones. The slowed-down ramp rates of package A and resistors decrease the temperature difference with package A before entering the reflow zone.

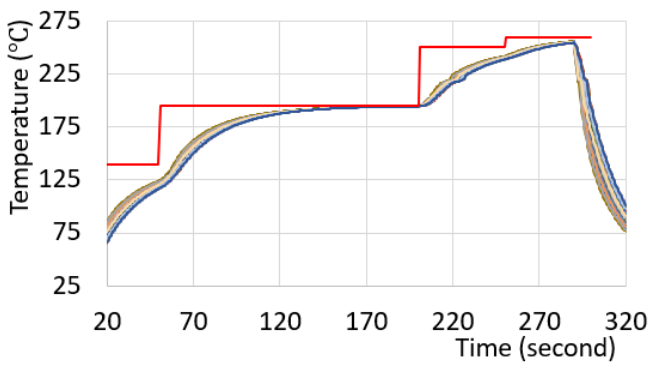

Fig. 16. Updated solder temperature of package B.

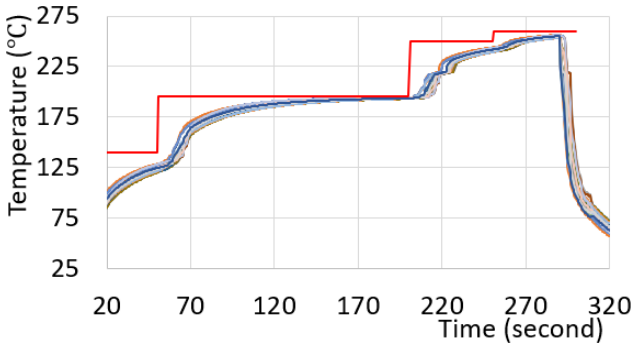

Fig. 17. Updated solder temperature of resistors.

TAL of resistors and package B are found different from those in the linear profiles. TAL in soak profile is reduced by 9–17 s which can relieve the risk of predried paste and excessive intermetallic layer growth [25]. This observation is similar to the result of Salam's study [26]. However, a gradual, linear profile brings less thermal shock than a ramp-soak-spike profile, which should be taken into consideration as well.

V. CONCLUSION

This article presents a methodology for developing a proper reflow profile for bulky BGA packages, which is harder to reach reflow temperature than small-size components. Temperature variation is found within the solder ball array. Hot spots are the solder joints at the peripheral, whereas cold spots are at the center or under the gap between the lid and die. To ensure complete solder paste melting and solidification, the minimum reflow temperature needs to be reached at the cold spot.

To eliminate thin and small features which are not practical for board-level models, the compact model methodology for BGA packages is introduced to simplify the CFD model used in the study. With the error analysis for different simplification methods, it is recommended to divide packages into three portions, i.e., lid and molding compound, core portion, and substrate.

After obtaining a proper reflow profile for BGA packages, a board-level simulation is conducted to inspect the compatibility of varied sizes of components being reflowed simultaneously. If overheating is not observed among components with a small thermal mass, the oven temperature setting is

qualified to reflow the complete board. Linear ramp profiles are compared with soak profiles. Shorter TAL in soak profiles is beneficial to relieve the risk of predried paste and excessive IMC growth. The extra thermal shock brought by soak profiles is also a considerable factor in profile selection.

Using this method, process engineers can quickly and smartly obtain the oven temperature settings for achieving the desired reflow profiles.

REFERENCES

[1] B. Illés and G. Harsányi, "Heating characteristics of convection reflow ovens," *Appl. Thermal Eng.*, vol. 29, nos. 11–12, pp. 2166–2171, Aug. 2009, doi: 10.1016/j.applthermaleng.2008.10.014.

[2] A. M. Najib, M. Z. Abdullah, C. Y. Khor, and A. A. Saad, "Experimental and numerical investigation of 3D gas flow temperature field in infrared heating reflow oven with circulating fan," *Int. J. Heat Mass Transf.*, vol. 87, pp. 49–58, Aug. 2015, doi: 10.1016/j.ijheatmasstransfer.2015.03.075.

[3] C. Lau, M. Z. Abdullah, and F. C. Ani, "Three-dimensional thermal investigations at board level in a reflow oven using thermal-coupling method," *Soldering Surf. Mount Technol.*, vol. 24, no. 3, pp. 167–182, Jun. 2012, doi: 10.1108/09540911211240038.

[4] K. Pan, J. H. Ha, H. Y. Wang, V. Veeraraghavan, and S. B. Park, "The effect of solder paste volume on surface Mount assembly self-alignment," *Proc. Manuf.*, vol. 38, pp. 1381–1393, Jan. 2019, doi: 10.1016/j.promfg.2020.01.150.

[5] J. Ha, K. Pan, H. Wang, D. H. Won, and S. B. Park, "The effect of misaligned passive component on fatigue life of solder joints and solder shape," in *Proc. 19th IEEE Intersoc. Conf. Thermal Thermomech. Phenomena Electron. Syst. (ITherm)*, Jul. 2020, pp. 1029–1034, doi: 10.1109/ITherm45881.2020.9190328.

[6] P. Yin, H. Wang, J. Xu, V. Pham, and S. Park, "Shock performance enhancement of a container for rack server," in *Proc. 19th IEEE Intersoc. Conf. Thermal Thermomech. Phenomena Electron. Syst. (ITherm)*, Jul. 2020, pp. 1264–1270, doi: 10.1109/ITherm45881.2020.9190277.

[7] C. Cai, K. Pan, J. Yang, and S. Park, "Comparative analysis of package warpage using confocal method and digital image correlation," in *Proc. 19th IEEE Intersoc. Conf. Thermal Thermomech. Phenomena Electron. Syst. (ITherm)*, Jul. 2020, pp. 945–949, doi: 10.1109/ITherm45881.2020.9190235.

[8] W. H. Zhong, Y. C. Chan, M. O. Alam, B. Y. Wu, and J. F. Guan, "Effect of multiple reflow processes on the reliability of ball grid array (BGA) solder joints," *J. Alloys Compounds*, vol. 414, nos. 1–2, pp. 123–130, Apr. 2006, doi: 10.1016/j.jallcom.2005.07.047.

[9] J. Xu, C. Cai, V. Pham, K. Pan, H. Wang, and S. Park, "A comprehensive study of electromigration in lead-free solder joint," *Proc. Electron. Compon. Technol. Conf.*, Jun. 2020, pp. 284–289, doi: 10.1109/ECTC32862.2020.00054.

[10] V. Wirth, K. Rendl, and F. Steiner, "Effect of multiple reflow cycles on intermetallic compound creation," in *Proc. 38th Int. Spring Seminar Electron. Technol. (ISSE)*, May 2015, pp. 226–230, doi: 10.1109/ISSE.2015.7247995.

[11] A. Esfandyari, B. Bachy, S. Raithel, A. Syed-Khaja, and J. Franke, "Simulation, optimization and experimental verification of the over–pressure reflow soldering process," *Proc. CIRP*, vol. 62, pp. 565–570, Jan. 2017, doi: 10.1016/j.procir.2016.06.092.

[12] T.-N. Tsai, "Modeling and optimization of reflow thermal profiling operation: A comparative study," *J. Chin. Inst. Ind. Eng.*, vol. 26, no. 6, pp. 480–492, Jan. 2009, doi: 10.1080/10170660909509162.

[13] Y. Lai, K. Pan, J. Xu, J. Yang, and S. Park, "Determination of smarter reflow profile to achieve a uniform temperature throughout a board," in *Proc. 20th IEEE Intersoc. Conf. Thermal Thermomech. Phenomena Electron. Syst. (iTherm)*, Jun. 2021, pp. 911–916, doi: 10.1109/ITherm51669.2021.9503258.

[14] Y. Lai *et al.*, "An intelligent system for reflow oven temperature settings based on hybrid physics-machine learning model," *Soldering Surf. Mount Technol.*, 2022, doi: 10.1108/ssmt-10-2021-0063.

[15] C.-S. Lau, M. Z. Abdullah, and F. C. Ani, "Computational fluid dynamic and thermal analysis for BGA assembly during forced convection reflow soldering process," *Soldering Surf. Mount Technol.*, vol. 24, no. 2, pp. 77–91, 2012, doi: 10.1108/09540911211214659.

[16] S. Shao *et al.*, "Comprehensive study on 2.5D package design for board-level reliability in thermal cycling and power cycling," in *Proc. IEEE 68th Electron. Compon. Technol. Conf. (ECTC)*, May 2018, pp. 1668–1675, doi: 10.1109/ECTC.2018.00251.

[17] S.-S. Deng, S.-J. Hwang, and H.-H. Lee, "Temperature prediction for system in package assembly during the reflow soldering process," *Int. J. Heat Mass Transf.*, vol. 98, pp. 1–9, Jul. 2016, doi: 10.1016/j.ijheatmasstransfer.2016.03.008.

[18] D. Straubinger, I. Bozsóki, D. Bušek, B. Illés, and A. Géczy, "Modelling of temperature distribution along PCB thickness in different substrates during reflow," *Circuit World*, vol. 46, no. 2, pp. 85–92, Dec. 2019, doi: 10.1108/CW-07-2019-0074.

[19] G. Refai-Ahmed *et al.*, "Lidless and lidded flip chip packages for advanced applications," in *Proc. IEEE 22nd Electron. Packag. Technol. Conf. (EPTC)*, Dec. 2020, pp. 104–111, doi: 10.1109/EPTC50525.2020.9315021.

[20] C. J. M. Lasance, "Ten years of boundary-condition- independent compact thermal modeling of electronic parts: A review," *Heat Transf. Eng.*, vol. 29, no. 2, pp. 149–168, Feb. 2008, doi: 10.1080/01457630701673188.

[21] C. Chen *et al.*, "Characterization of after-reflow misalignment on head-in-pillow defect in BGA assembly," in *Proc. 15th Int. Conf. Electron. Packag. Technol.*, May 2014, pp. 1177–1180, doi: 10.1109/ICEPT.2014.6922853.

[22] K. Dusek, C. Stancu, P. V. Notingher, P. Mach, and M. Placek, "Experimental and numerical analysis of melting and solidification of SnAgCu joints," *IEEE Trans. Compon., Packag., Manuf. Technol.*, vol. 6, no. 9, pp. 1445–1455, Sep. 2016, doi: 10.1109/TCPMT.2016.2593709.

[23] H. Yu, T. T. Mattila, and J. K. Kivilahti, "Thermal simulation of the solidification of lead-free solder interconnections," *IEEE Trans. Compon. Packag. Technol.*, vol. 29, no. 3, pp. 475–485, Sep. 2006, doi: 10.1109/TCAPT.2005.848590.

[24] *Indium8.9HF Pb-Free Solder Paste 98485 R15*, document 98485, I. Corporation, 2018, pp. 8–9.

[25] K. Pan, J. H. Ha, H. Wang, J. Xu, and S. Park, "An analysis of solder joint formation and self-alignment of chip capacitors," *IEEE Trans. Compon., Packag., Manuf. Technol.*, vol. 11, no. 1, pp. 161–168, Jan. 2021, doi: 10.1109/TCPMT.2020.3034211.

[26] B. Salam, C. Virseda, H. Da, N. N. Ekere, and R. Durairaj, "Reflow profile study of the Sn-Ag-Cu solder," *Soldering Surf. Mount Technol.*, vol. 16, no. 1, pp. 27–34, Apr. 2004, doi: 10.1108/09540910410517022.

Yangyang Lai (Graduate Student Member, IEEE) received the M.S. degree in mechanical engineering from the State University of New York at Binghamton, Binghamton, NY, USA, in 2021, where he is currently pursuing the Ph.D. degree.

His current research interests include the optimization of reflow soldering using hybrid numerical and machine learning approaches, and accessing the thermal reliability of electronic packages.

Ke Pan (Graduate Student Member, IEEE) received the B.S. degree in power and energy engineering from the Wuhan University of Technology, Wuhan, China, in 2017. He is currently pursuing the Ph.D. degree in mechanical engineering with the Opto-Mechanics and Physical Reliability Laboratory, State University of New York at Binghamton, Binghamton, NY, USA.

He is also concentrating on design advanced experiment methods for accessing the mechanical and thermal reliability of microelectronic packages.

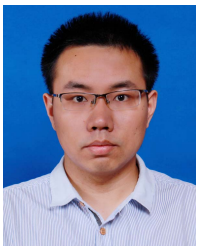

Chongyang Cai received the B.S. and M.S. degrees from the Harbin Institute of Technology, Harbin, China, in 2016 and 2018, respectively. He is currently pursuing the Ph.D. degree in mechanical engineering with the Opto-Mechanics and Physical Reliability Laboratory, State University of New York at Binghamton, Binghamton, NY, USA.

His research interests include low melting temperature solder reliability under thermal cycling and electromigration.

Pengcheng Yin received the B.S. degree in mechanical design and manufacture and its automation from the Central South University of Forestry and Technology, Changsha, China, in 2018, and the M.S. degree in mechanical engineering from the State University of New York at Binghamton, Binghamton, NY, USA, in 2020, where he is currently pursuing the Ph.D. degree in mechanical engineering with the Opto-Mechanics and Physical Reliability Laboratory.

He is also concentrating on design dynamic impact experiments and shock/impact/vibration simulation of electronic packaging.

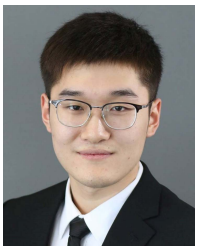

Junbo Yang received the B.S. degree in process equipment and control engineering from the Beijing University of Chemical Technology, Beijing, China, in 2017, and the M.S. degree in mechanical engineering from the State University of New York at Binghamton, Binghamton, NY, USA, in 2019, where he is currently pursuing the Ph.D. degree with the Opto-Mechanics and Physical Reliability Laboratory, Department of Mechanical Engineering.

His current research interests include experiments and simulation to improve the reliability of microelectronics packaging.

Seungbae Park (Senior Member, IEEE) received the Ph.D. degree from Purdue University, West Lafayette, IN, USA, in 1994.

He was with IBM, Armonk, NY, USA, as a Development and Reliability Engineer, where he was responsible for flip-chip technology. Since 2002, he has been a Professor with the Department of Mechanical Engineering, State University of New York at Binghamton, Binghamton, NY, USA. He is currently the Director of the Binghamton University's Integrated Electronics Engineering Center (IEEC). His current research interests include physical reliability for microelectronics and microelectromechanical systems packaging.

Dr. Park is also a fellow of the American Society of Mechanical Engineers (ASME). He has served many technical communities. He was the Chair of the iNEMI's Modeling and Simulation Technical Work Group and the Electronics Packaging Council in the Society of Experimental Mechanics.